Coupled thermo-mechanical numerical modelling of carbon fibre reinforced composites impacted with different projectile configurations

ISBN number: 978-1-925627-66-4
Please select category below:
Normal Paper ☒
Student Paper ☐
Young Engineer Paper ☐

Coupled thermo-mechanical numerical modelling of carbon fibre reinforced composites impacted with different projectile configurations

A. Polla[1,2], G. Frulla[1], E. Cestino[1], R. Das[2] and P. Marzocca[2]

[1]*Department of Mechanical and Aerospace Engineering (DIMEAS), Politecnico di Torino, Torino, Italy*
[2]*Sir Lawrence Wackett Defence and Aerospace Centre, RMIT University, Melbourne, Australia*

Abstract

A key challenge in building a predictive numerical model for composite structures is the ability to accurately characterize their failure behaviour, especially under impact loading. In this paper, a coupled thermo-mechanical modelling technique and the associated numerical simulations of carbon fibre-reinforced composite panels under the high-velocity impact (HVI) are introduced. The modelling technique aims to evaluate the progressive damage failure analysis (PDFA) of a flat composite panel made of T800/F3900 unidirectional carbon fibre and epoxy, with 16-ply in a quasi-isotropic layup configuration [(0/90/45/-45)2]$_S$. Mechanical characterization test data of the proposed composite materials have been obtained from FAA experimental campaign. High fidelity complete stacked shell-cohesive method is implemented to evaluate composite delaminations and intralaminar damage. The heat generated due to the projectile kinetic energy and impact-induced damage energy transformation is investigated with the proposed numerical coupled model. Thermal effects on the mechanical performance of composite targets are investigated based on the application of the constitutive transient thermal coupling method available in LS-DYNA®. Moreover, the explicit dynamic finite element analysis presented considers four characteristic aerospace projectiles to compare the development of the damage generated during normal high-velocity impact events. The impact response results of the selected projectile configurations, including rubber cylindrical projectile, bird-like projectile, CFRP composite platelike projectile, and ASTM D8101 aluminium axisymmetric projectile, are compared. Impactors with equivalent kinematic energy are investigated with emphasis on energy transfer mechanisms and the local projectile-induced target deformation, damage, and failure. The study introduces the proposed modelling techniques, energy transfer phenomenon, and damage mechanisms that are observed in the target plates. The proposed numerical technique will be used in future research works to investigate engine bird-strike events and the consequently Fan Blade-Out (FBO) scenario to increase the reliability of aerospace structures and to improve the design numerical methods.

Keywords: Aerospace composites, high-velocity impact, thermal analysis.

Introduction

The development of reliable advanced computational analysis methods is a key factor to reduce the design and certification timeline for new composite structures used in aeronautics applications. The main purpose of the NASA Advanced Composite Project (ACP) was to develop a reliable physical-based modelling methodology to evaluate High Energy Dynamic Impact events over composite structures [1]. A convergence of several specific tools is necessary to achieve the goal of obtaining this complex framework for the evaluation of composite structures when subjected to high dynamic load. Specific constitutive material models are necessary to physically describe the elastic and fracture evolution of selected materials within a reliable modelling technique. Several studies have been conducted by NASA to characterize and reproduce the experimental observations with different proposed numerical solutions and material models [2]–[4]. A significant amount of high-velocity impact testing has been performed for several composite structures with selected fibre architectures. For this reason, the ASTM D8101 [5] have been developed to standardize the penetration resistance of composite materials for aerospace applications. In this paper, a coupled thermo-mechanical modelling technique is introduced for the evaluation of carbon fibre-reinforced composite panels subjected to high-velocity impacts (HVI). Moreover, a validated high-fidelity complete stacked shell-cohesive method has been implemented to evaluate delaminations and intralaminar damage of a composite panel when impacted by four different characteristic aerospace projectiles.

Progressive Damage Failure Analysis

A square unidirectional T800/F3900 composite panel with 16-ply in a quasi-isotropic layup configuration $[(0/90/45/-45)2]_S$ and planar dimensions of 305 x 305 mm with a global thickness of 3.1mm is modelled. An extensive experimental test campaign has been achieved by FAA and NASA to define the elastic and failure mechanical properties of the selected composite material [6], [7]. The composite panel geometry and dimensions are based on the ASTM D8101 standard [5] with a cylindrical clamping section with an internal radius of 127mm and an external radius of 153mm. The boundary conditions have been modelled by single-point constraints (SPC). The bolts region was simulated by constraining the in-plane displacement, while the top and bottom nodes of the composite panel within the cylindrical rigid frame were constrained in the out-of-plane direction (Figure 1). A structured mesh has been selected for the central circular section of the panel with a minimum mesh size of 1mm. A complete stacked shell modelling technique (L2DE-Cohesive) has been proposed as described by Polla et al. [8], [9]. A single plane of 2D shell elements is introduced for each composite ply belonging to the selected laminate positioned at its mid-surface. CZM elements (Cohesive Zone Model) guarantee structural continuity through the thickness being properly connected node-to-node to the adjacent ply mesh structure. Specific LS-DYNA automatic surface-to-surface algorithm was employed to define ply-to-ply post-failure interaction and to reproduce the Coulomb friction that exists between delaminated ply interfaces. Equivalent contact algorithms have been adopted also to model the dynamic interaction between the selected projectile and the composite plies modelled. LS-DYNA material formulation MAT58 and MAT138 have been adopted respectively for the characterization of the intralaminar and interlaminar material behaviour. The specific numerical parameters adopted for the presented modelling technique will be described in detail in further research articles.

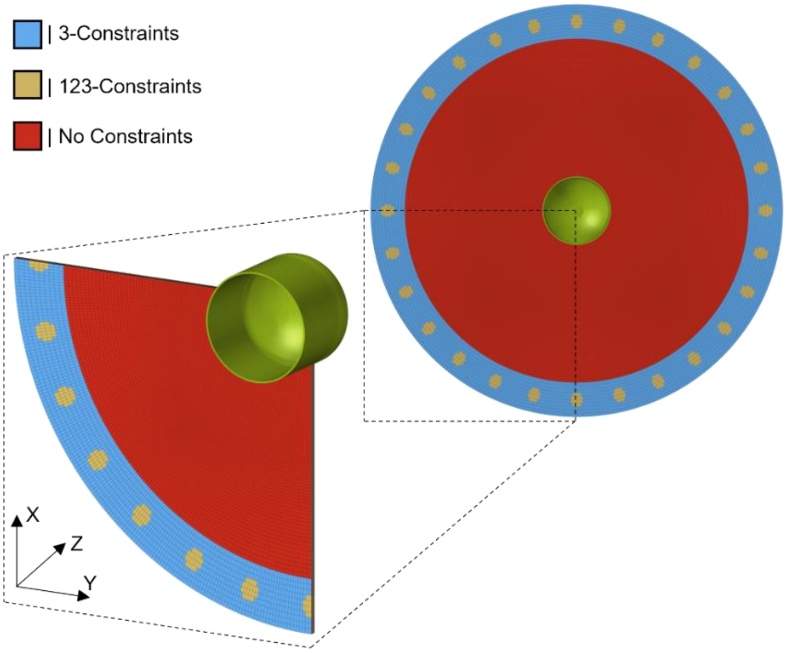

Figure 1. Boundary condition and structured mesh structure of the selected composite panel.

The presented numerical modelling technique has been calibrated with the experimental evidence described in the last NASA ACP research projects [1]–[4] and [10]. Post-failure parameters have been selected to correctly reproduce the physical observations. The ballistic qualitative and quantitative results obtained with the impact of the ASTM D8101 rigid impactor at 127m/s against the selected composite panel are reported in Figure 2 and Figure 3. The numerical fracture morphology with also the delamination shape and relative extension is compared against the experimental data summarized in [10]. The residual velocity of the ASTM projectile after the complete perforation of the composite panel oscillates around 11.41-14.16 m/s which is perfectly congruent with what is reported in [10] (Figure 4). The introduced modelling technique [8] has been used for the evaluation of the coupled thermal-structural solution in the same dynamic condition.

Coupled thermo-mechanical model

A high-velocity impact scenario is considered a thermodynamically adiabatic evolution process. The dynamic phenomenon is typically completely extinguished in less than 5ms. The internal heat generated due to the conversion of the kinematic energy (KE) of the projectile and the contact friction into the internal fracture energy (IE) is stored completely internally inside the impacted composite structure. No consistent conduction is present between the impacted structure and the external environment. Several studies in the literature have used IR cameras to evaluate the variation of the temperature inside composite panels when subjected to high-speed impact. The results show that temperatures above 202°C were generated internally during impact [11], [12]. A high internal temperature gradient can change the physical and mechanical conditions of materials present inside the structure and modify the material dynamic evolution process as it is approaching the typical glass transition temperature for aerospace-grade epoxy resins.

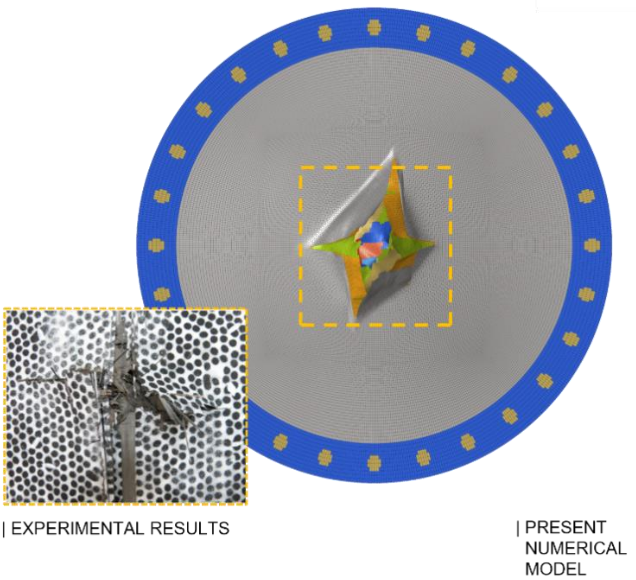

Figure 2. Fracture morphology obtained with the application of the selected numerical modelling technique in comparison with the experimental evidence.

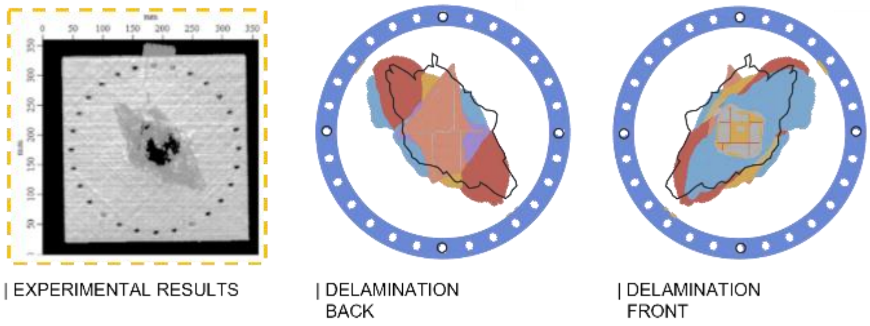

Figure 3. Numerical evaluations of proposed modelling technique against experimental evidence: SX – Fracture external morphology; DX – Delamination shape and extension.

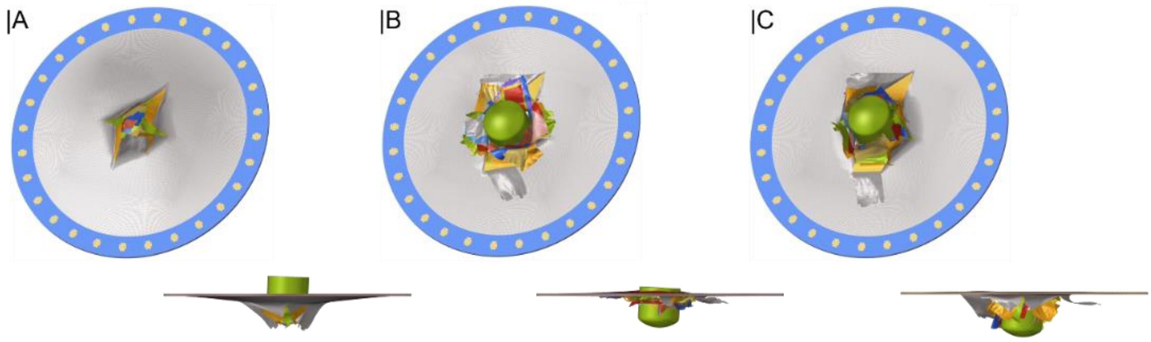

Figure 4. ASTM D8101 projectile at 127m/s induced damage: A – 0.5ms; B – 1.5ms; C – 2.5ms;

A specific LS-DYNA thermo-mechanical analysis has been performed to evaluate the thermal gradient observed internally in each ply in the indicated test conditions. Principal thermal-structural characteristic material properties necessary for the specified simulation have been extracted from the literature [13]–[16]. Figure 5 reports the temperature distribution for each composite layer at 25% resulting projectile initial KE. The thermal gradient distribution through the thickness and around the active fracture zone (AFZ) is reported. Max temperature values are localized in the central layer also due to the low thermal conduction of the CFRP and related to the maximum through-thickness interlaminar stresses generated during the orthogonal impact.

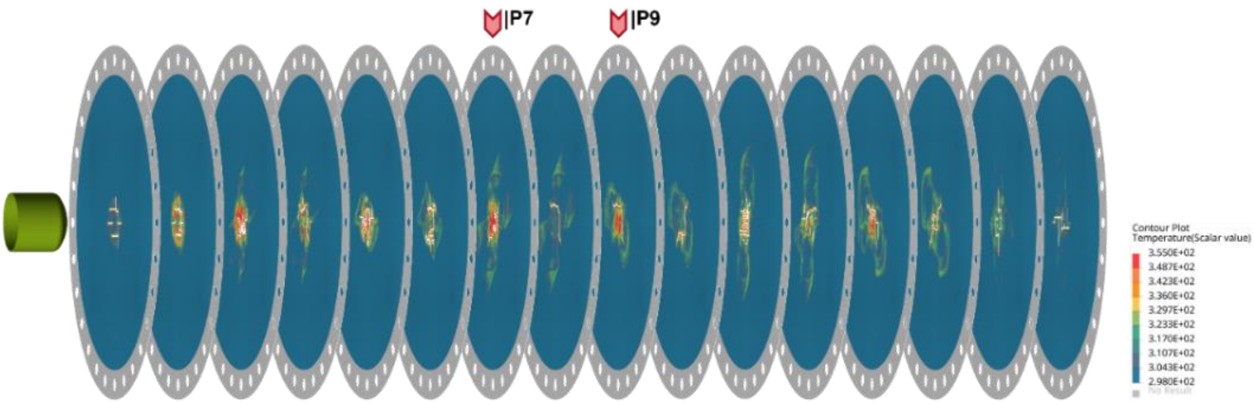

Figure 5. Global thermal load at 2ms for all the composite plies; Axisymmetric flat projectile in green. Selected composite layers P7 & P9 are highlighted in the flat panel stratification.

In particular, ply P7 & P9 temperature maps are reported in Figure 6: the observed localized peak temperature is around 187°C above the typical epoxy glass transition temperature that ranges respectively around 80°C - 150°C for resin infusion and pre-pregs resins. Such thermal effects numerically determined have been investigated in particular for the related resin infusion (RI) characteristic material limitations previously introduced. The thermal load between 25-82°C is divided into four specific regions. Each characteristic temperature range associated with the plies P7 and P9 is reported in Figure 6. Each section represents a specific range of temperature that for the resin adopted for the RI process can set a progressive reduction of the associated mechanical properties.

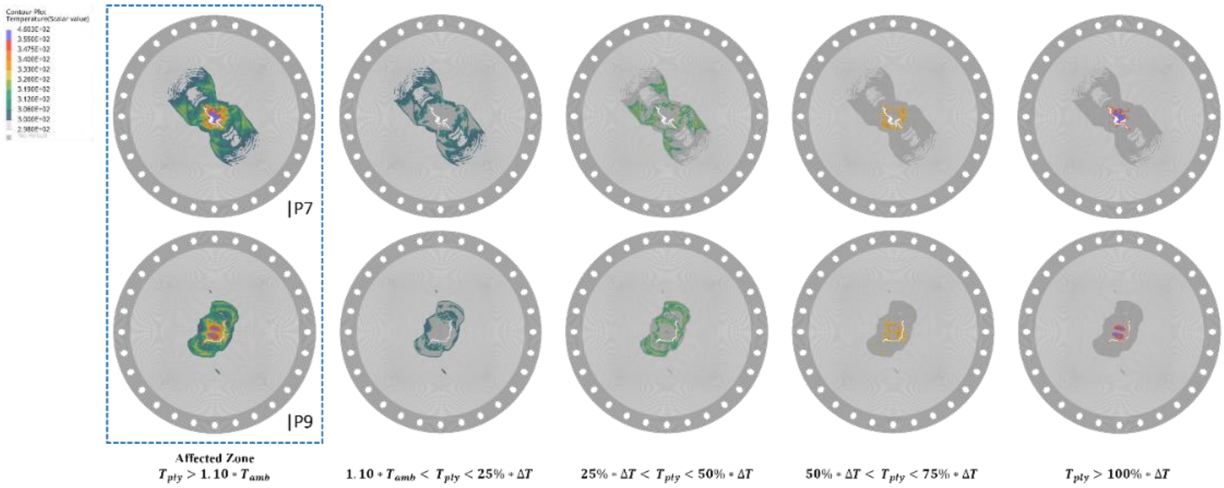

Figure 6. Specific temperature distribution for two selected composite plies (P7 & P9)

Characteristic aerospace projectiles performances

Three different architecture and material combinations have been evaluated as previously introduced (Figure 7) with the same external maximum diameter of the impactors.

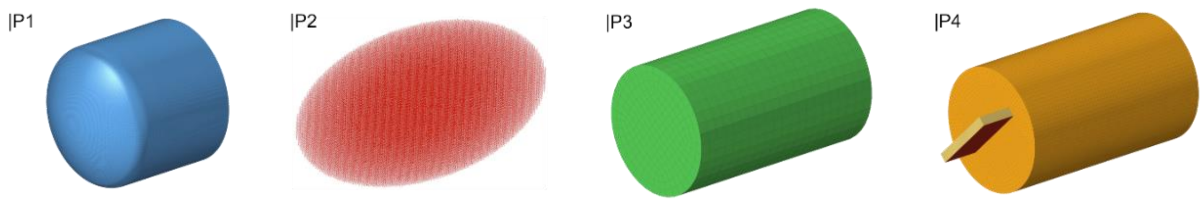

Figure 7. Selection of certified projectiles for aerospace applications: P1 – ASTM; P2 – SPH Bird; P3 – Lagrangian Rubber; P4 – Composite plate-like.

The selected impactor configurations try to cover all the standardized applications that have been found in the literature and in the FAA best-practice procedures: a bird-like projectile (P2) used for the certification of aeronautical engines simulated by a Smoothed-Particle Hydrodynamics (SPH) numerical technique; Rubber cylinder (P3) adopted for soft-body impact in Fan Blade out (FBO) simulated by a classical Lagrangian method in certification tests; a Composite plate-like model (P4) used to investigate fracture initiation associated with the impact of composite plate debris. Two different sets of analysis have been introduced for all the defined projectile configurations: 1) evaluation of the impact effect of the selected projectile's architecture with the same kinematic energy as in [9]; 2) comparison of the ballistic velocity diagram of each projectile with the same initial velocity against the original ASTM results.

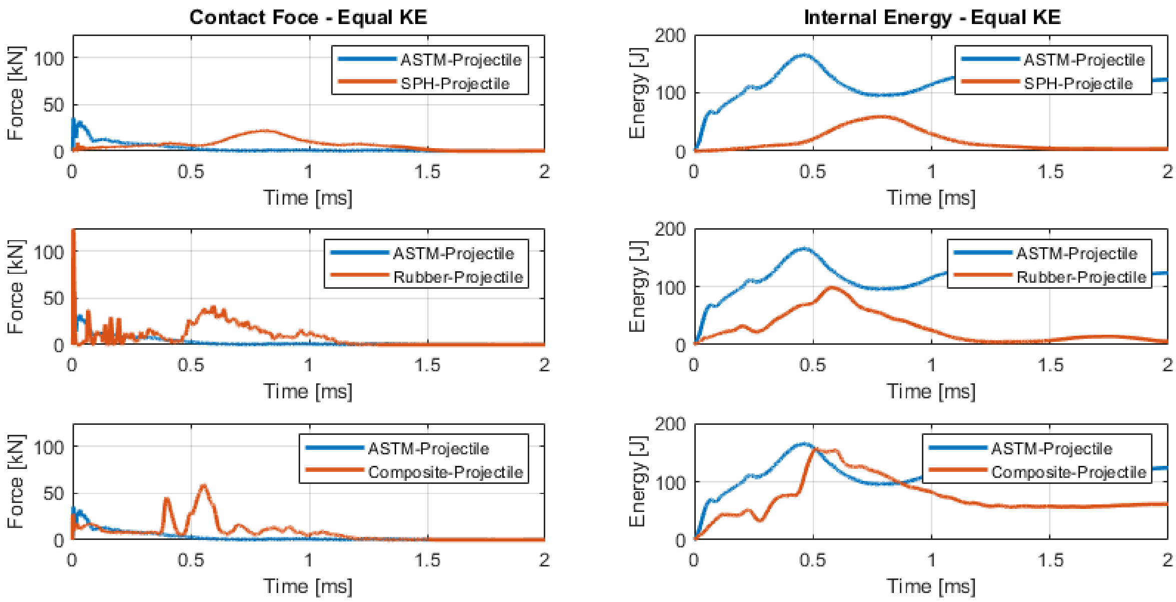

Figure 8. Equal kinematic energy comparison: SX – Contact force of proposed projectile configurations; DX – Internal energy of proposed projectile configurations.

Figure 8 shows that the contact peak load generated with the ASTM projectile is typically higher than what is observed for the other proposed projectile configurations in the first few milliseconds (less than 0.5ms). For the other proposed projectiles (the same equivalent initial KE), the peak in the contact load is observed between 0.5-1ms. Internal energy is compared for all the defined groups against the numerical results obtained with the standardized ASTM projectile. The conversion of the KE into fracture internal energy is more effective for the flat rigid ASTM impactor in comparison to the others. The amount of energy dynamically absorbed by composite structure has been evaluated using standardized projectile geometry. The ballistic graph of the introduced set of projectiles with the same initial velocity is presented in Figure 9. Figure 10 shows the fracture morphology at 2.5ms related to all the impactors compared to the results obtained in Figure 4. The ASTM projectile set the highest reduction of the KE in the initial 0.6ms of impact evolution. The stress distribution for the ASTM standardized impactor is bigger than the other projectile configurations as already indicated.

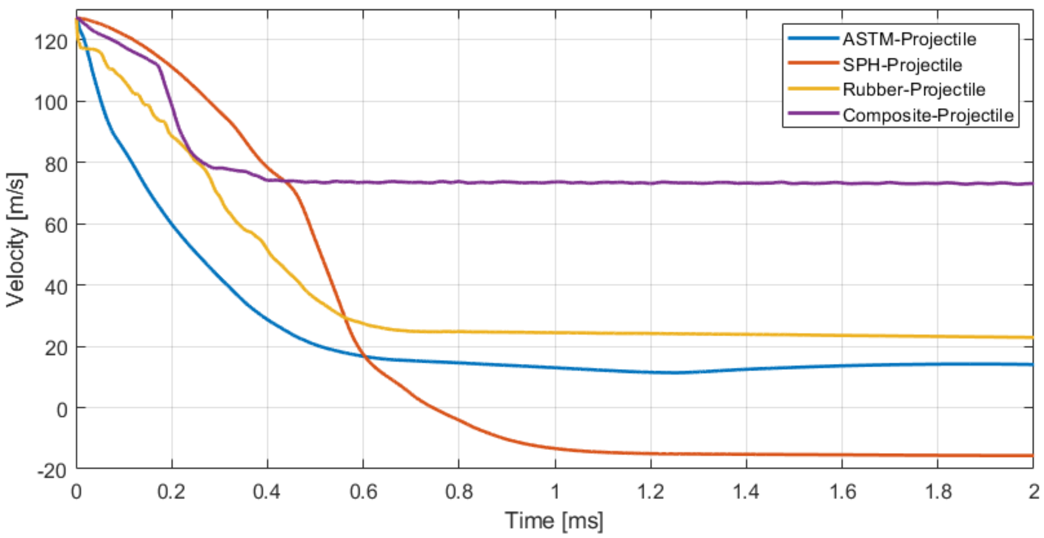

Figure 9. Comparison of projectile velocity evolution for the proposed projectile configurations.

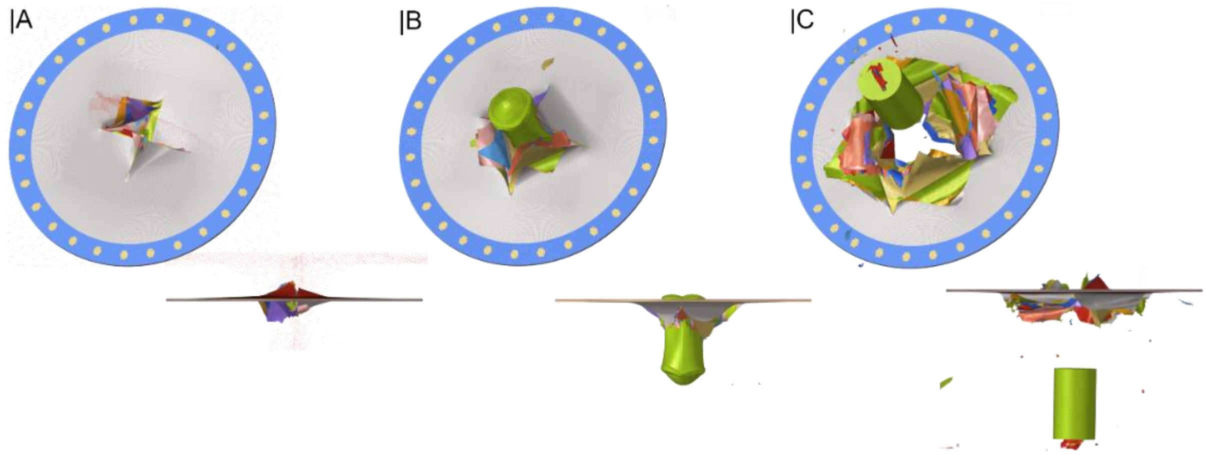

Figure 10. Comparison of fracture morphology at 2.5ms: A – Bird-Like; B – Rubber Cylinder; C – Composite Plate;

Conclusions

A high-fidelity complete stacked shell-cohesive modelling technique has been applied to numerically evaluate the thermal-structural coupled effect associated with the impact of high-velocity projectiles against a laminated composite structure. The thermal load generated with the conversion of the kinetic energy and the contact friction can cause a severe reduction of the mechanical properties of the interlaminar epoxy resin that constitutes the CFRP structure. Moreover, the ballistic performances of selected aerospace-grade projectiles have been compared against the results obtained with the ASTM projectile configuration. Two specific sets of analyses have been conducted: equivalent KE and equivalent initial velocity. In both the presented sets the ASTM projectile is always capable to define the highest stress concentration inside the composite structure. It can be observed that in both sets of simulations, the IE peak and the KE reduction associated with the ASTM standard are always higher than the other type of projectiles. The results reported show also the comparison between the fracture morphology obtained through the application of selected impactors geometry. The proposed numerical technique and the impactor models introduced in the LS-DYNA solutions will be used for the evaluation of a bird strike event and the consequent Fan Blade-Out scenario to increase the reliability of aerospace components.

References

[1] M. Melis, M. Pereira, R. K. Goldberg, and M. Rassaian, ‘Dynamic Impact Testing and Model Development in Support of NASA’s Advanced Composites Program’, in *2018 AIAA/ASCE/AHS/ASC Structures, Structural Dynamics, and Materials Conference*, Kissimmee, Florida, Jan. 2018. doi: 10.2514/6.2018-1699.

[2] K. J. Hunziker, J. Pang, M. Pereira, M. Melis, and M. Rassaian, ‘NASA ACC High Energy Dynamic Impact Methodology and Outcomes’, in *2018 AIAA/ASCE/AHS/ASC Structures, Structural Dynamics, and Materials Conference,* Kissimmee, Florida, Jan. 2018. doi: 10.2514/6.2018-1700.

[3] B. Justusson, J. Pang, M. Molitor, M. Rassaian, and R. Rosman, ‘An Overview of the NASA Advanced Composites Consortium High Energy Dynamic Impact Phase II Technical Path’, in *AIAA Scitech 2019 Forum,* San Diego, California, Jan. 2019. doi: 10.2514/6.2019-2052.

[4] A. D. Byar, J. K. Pang, J. Iqbal, J. Ko, and M. Rassaian, ‘Determination of Ballistic Limit for IM7/8552 Using LS-DYNA’, p. 11.

[5] D30 Committee, ‘Test Method for Measuring the Damage Resistance of a Fiber-Reinforced Polymer Matrix Composite to a Drop-Weight Impact Event’, ASTM International. doi: 10.1520/D7136_D7136M-15.

[6] United States. Department of Transportation. Federal Aviation Administration, Ed., ‘Development of a Tabulated Material Model for Composite Material Failure, MAT213 Part 2: Experimental Tests to Characterize the Behavior and Properties of T800-F3900 Toray Composite’, no. DOT/FAA/TC-19/50, P2, Jan. 2019, [Online]. Available: https://rosap.ntl.bts.gov/view/dot/57814

[7] N. Holt, B. Khaled, L. Shyamsunder, and S. D. Rajan, ‘T800-F3900 Composite Stacked Ply Laminate Testing and Modeling Using MAT_213’, no. DOT/FAA/TC-21/56, May 2022, doi: 10.21949/1524483.

[8] A. Polla, P. Piana, E. Cestino, and G. Frulla, ‘Delamination and Fracture Modeling Techniques for Shell Composite Structures in LS-DYNA®’, p. 12, 2021.

[9] A. Polla, G. Frulla, E. Cestino, R. Das, and P. Marzocca, ‘Numerical and Experimental structural characterization of composite advanced joint for ultra-light aerospace platform.’, presented at the 33rd ICAS Congress, Sep. 2022.

[10] L. Shyamsunder, B. Khaled, S. D. Rajan, J. M. Pereira, P. DuBois, and G. Blankenhorn, ‘Numerical validation of composite panel impact tests’, *Int. J. Impact Eng.*, vol. 159, p. 104032, Jan. 2022, doi: 10.1016/j.ijimpeng.2021.104032.

[11] M. Papantonakis, R. Furstenberg, and V. Nguyen, ‘Infrared imaging analysis of ballistic impacts of composite armor materials.’, presented at the Proceedings of SPIE 9105, Thermosense: Thermal Infrared Applications XXXVI, Baltimore, Maryland, May 2014, vol. p.91050B.

[12] F. Marcotte, S. Ouellet, and V. Farley, ‘Analysis of the ballistic impact response of a composite material using FAST infrared imagery.’, presented at the Proceedings of SPIE 8705, Thermosense: Thermal Infrared Applications XXXV, Baltimore, Maryland, May 2013, vol. p.870509.

[13] *Failure Criteria in Fibre-Reinforced-Polymer Composites*. Elsevier, 2004. doi: 10.1016/B978-0-080-44475-8.X5000-8.

[14] ‘Polymers - Specific Heats’. https://www.engineeringtoolbox.com/specific-heat-polymers-d_1862.html (accessed Feb. 01, 2023).

[15] ‘Metals - Specific Heats’. https://www.engineeringtoolbox.com/specific-heat-metals-d_152.html (accessed Feb. 01, 2023).

[16] ‘Emissivity Coefficients common Products’. https://www.engineeringtoolbox.com/emissivity-coefficients-d_447.html (accessed Feb. 01, 2023).